Alahmad *et al. BMC Oral Health* (2025) 25:659
https://doi.org/10.1186/s12903-025-05994-4

BMC Oral Health

RESEARCH Open Access

Enhancing PMMA properties: a comprehensive study of nanographene oxide and Boron nitride impact through In-Vitro analysis

Hessah Alahmad[1], Reem Alamir[1], Mohammad Asadzadeh[2], Umer Daood[3] and Syed Saad Bin Qasim[1*]

Abstract

Background Polymethylmethacrylate is a commonly used biomaterial in dentistry. Although the material have been used for several years it has some limitations with respect to physical and mechanical properties. Researchers are exploring the potential of novel nanomaterials like nanographene oxide (nGO) and hexagonal boron nitride (hBN) to be used as a reinforcing agent. Therefore, the current investigation sought to evaluated physical, chemical, mechanical and antimicrobial potential of PMMA reinforced with nGO and hBN alone and synergistically as well.

Methods Four different groups were prepared including the control group (G1)0.2.5 wt% nGO was added to the liquid component (G2), 1 wt% hBN was added to the powder component (G3) and 2.5 wt % nGO with 1 wt % hBN combined (G4.) The resulting nanocomposite were characterized using microhardness, flexural and compressive strength analysis, contact angle analysis and degree of conversion was also calculated using Fourier Transform Infrared spectroscopy. The antimicrobial efficacy was assessed against *Candida albicans*. Statistical analysis was performed to determine the difference between the groups. One-way ANOVA was performed followed by Tukey's post hoc test for multiple comparisons between the groups.

Results The addition of nGO (17.67 ± 2.41 HV) ($p > 0.001$) significantly increased the microhardness compared to the unmodified PMMA (15.91 ± 1.57 HV) ($p > 0.001$).The addition of both, nGO and hBN enhanced hydrophilicity (61.4° ± 2.36) and the surface roughness. Degree of conversion was found to be less than the control specimens for all experimental groups. G2 showed significantly less Candida albicans attachment compared to G1 ($p < 0.05$).

Conclusion The synergistic effect of nGO and hBN on PMMA shows promise for enhancing wettability and antimicrobial properties. However, the trade-off with lower polymerization conversion and increased roughness needs to be addressed. Future work could focus on optimizing the composition and processing conditions to maximize beneficial properties while minimizing negative impacts on physiochemical, mechanical performance and microbial adhesion.

Keywords Nanographene oxide, Hexagonal boron nitride, Acrylic, PMMA, Characterization

---

*Correspondence:
Syed Saad Bin Qasim
sayed.binqasim@ku.edu.kw
[1] Department of Bioclinical Sciences, College of Dentistry, Kuwait University, P.O. Box 24923, Kuwait City Safat-13110, Kuwait
[2] Department of Microbiology, Faculty of Medicine, Kuwait University, P.O. Box 24923, Kuwait City Safat 13110, Kuwait
[3] Restorative Dentistry Division, School of Dentistry, International Medical University Kuala Lumpur, 126, Jalan Jalil Perkasa 19, Bukit Jalil, 57000 Bukit Jalil, Wilayah Persekutuan, Kuala Lumpur, Malaysia

Introduction

Polymethylmethacrylate (PMMA) has been a biomaterial of choice in prosthodontics for decades [1]. Its utility in different medical and dental clinical applications has grown since its inception. Its physiochemical and mechanical of durability, dimensional stability, cost-effectiveness, aesthetics and ease of fabrication position it favorably compared to alternate biomaterials used for similar applications [2]. Specifically its properties are harnessed to fabricate fixed and removeable dental prosthesis. Other applications also include their use as bone cements and facial prosthesis [3]. Despite the acceptable properties, it is prone to fracture due to multiple reasons [4]. Another drawback is the poor antimicrobial property, whereby their prolonged usage can cause fungal infection when in contact with oral tissues [3]. Moreover, long term exposure to saliva makes the denture base acrylic resin susceptible to aging and may promote oral diseases [1]. To overcome these hurdles, bioactive glasses [5], glass fibers [6] and more recently nanomaterials (nanoparticles, nanosheets, and nanotubules) are being explored by investigators across the globe as fillers to reinforce the existing properties [1, 2, 7].

The use of these different strategies is targeted mainly at improving the performance of denture base resin. Therefore, reinforcement with nanoparticles [2], nanofibers and mesoporous silica [1] are still an area of interest. Amongst the nanoparticles frequently studied are silver [8], titanium dioxide [2], zirconium dioxide [9], graphene oxide [3, 10, 11] and boron nitride [12]. Graphene based materials like reduced graphene oxide and graphene platelets are gaining more attention as PMMA additives due to their high surface area, biocompatibility, conductivity, strength, low density and ease of modification [3, 10]. Graphene exists as a single atomic plane of carbon in the form of a honeycomb lattice [13]. Graphene oxide is a highly oxidized from of graphene prepared by oxidation of graphite. This amphiphilic compound has reactive oxygen functionalities which allow for functionalization hence, increasing their interest to use nGO as an additive in existing biomaterials [14]. Different concentrations and formulations have been studied [3, 10, 15, 16]. A disadvantage of nGO is its dark color change at higher concentrations. Nevertheless, these reinforced biomaterials can be used in the palatal area, where denture stomatitis is more common [15]. Whilst nanoparticles have been reported to exhibit several advantages there are some limitations that also need to be taken into account. Their toxicity, carcinogenicity and teratogenicity also needs to be evaluated. In most of the applications they are used below their threshold concentrations. Furthermore, if nanoparticles are used for an extended time period there are chances of bioaccumulation inside body [17]. Hexagonal boron nitride (hBN), also known as "white graphene", is a two-dimensional nanomaterial that has similar chemical structure and properties to graphene [18, 19]. Its inherent white color makes hBN incorporation into dental biomaterials a potential solution to counteract the darkening caused by nGO, more specifically at weight percentages. Moreover, its properties such as biocompatibility, antibacterial effect, and high surface area have been harnessed for its use as an additive in dental biomaterials [18]. Whilst nGO and hBN have been investigated in the literature individually, research literature on their synergistic effects remains limited [20, 21].

Therefore, the aim of the current study is to investigate the effect nGO and hBN alone and in combination as nanofillers in self-cured PMMA in comparison to pure PMMA (control), in an attempt to reinforce its physiochemical, mechanical properties. The null hypothesis was that the addition of nGO, hBN alone or in combination with will have no effect on the physical, chemical and mechanical properties of commercially available self-cure PMMA resin.

Materials and methods

Materials

Self or Cold Poly Methyl Methacrylate (PMMA) (Interdent, Interacryl Cold, Slovenia), Ultra Highly Concentrated Single-Layer Graphene Oxide (nGO) (Color: brown; concentration: 6.2 g/L; and flake size: 0.5 to 5 μm) (Graphene Supermarket®, Graphene Laboratories Inc., Ronkonkoma, NY, USA), Boron Nitride nanopowder (BN) (< 150 nm, USA, Sigma aldrich MA, USA). The molds were prepared at the biomedical engineering department of Health Science center, Kuwait University. A schematic representation of the groups made and characterizations done are displayed in Fig. 1.

Preparation of the samples

The samples of the control group (G1) were prepared according to the manufacturer instructions by hand mixing the PMMA powder to the liquid at a powder to liquid ratio of 1.3:1. 13 g of powder was weighed on a digital measuring balance (CG 2202 C Citizen) and added to 10 ml of liquid. The solution was manually mixed with a stainless-steel spatula in a rubber bowl until it achieved a soft dough-like consistency. Subsequently, the mixture was promptly poured into molds designed for each specific test and compressed between two glass slides. Prior to pouring, a thin layer of petroleum jelly (Vaseline®, Unilever, Englewood Cliffs, NJ) was applied to the molds. After the setting time, which was mentioned in the manufacturer's manual, was reached, the samples were removed from the molds. For the preparation of group 2 (G2), 2.5 wt % Nanographene Oxide (nGO) was incorporated into the PMMA liquid homogenously under sonication for 1 h according to the literature [3].

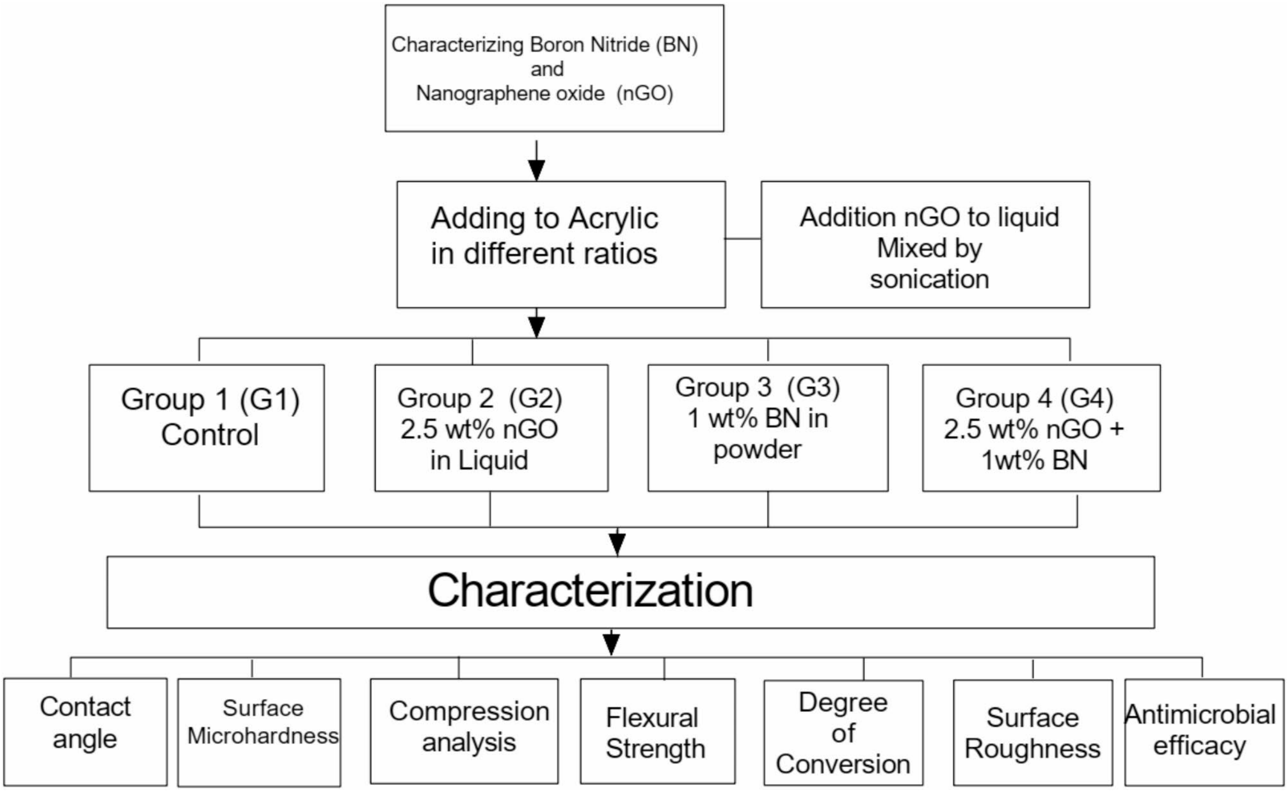

Fig. 1 A schematic flow chart representing the study design. G1 is control, G2 is reinforced with 2.5 wt % nGO, G3 is loaded with 1 wt % hBN and G4 is mixed with 2.5 wt% nGO and 1 wt% hBN

The liquid was then hand mixed with the PMMA powder. The samples of group 3 (G3) were prepared by incorporating 1 wt % Boron Nitride (hBN) to the PMMA powder and then hand mixed with the PMMA liquid. Group 4 (G4) were prepared samples were prepared by adding 2.5 wt % nGO to the PMMA liquid, under sonication for 1 h as described previously of G2 and adding 1 wt % hBN to the PMMA powder. Samples of all groups were polished with Silicon carbide (SiC) papers (220, 400, 600, 1000 grit CArbiMet, Bueler, Lake Buff, IL, USA) and stored in distilled water at 37 ± 2 °C in an incubator for a duration of 24 h prior to characterization.

Mechanical characterization

Disk-shaped acrylic molds (10 ± 0.5 mm diameter and 2 ± 0.5 mm thickness) were fabricated to prepare the specimens for microhardness testing ($n = 10$). Microhardness was conducted on a digital microhardness tester with a load cell of 50 g and indentation time for 20 s on the surface of the specimen with a Vickers diamond indentor (CV Instruments 400DAT/3) at room temperature (25 °C). The average value of 10 randomly selected points in each sample was taken into account for further analysis. Diagonal lengths of the indentations was measured with an objective lens of 40×. Microhardness in g / μm^2 was calculated from the following Eq. 1:

$$HV = 1.854\,F/D2 \tag{1}$$

Where HV = Vickers Hardness, F = load set in kilograms (kg), and d = diagonal's length in mm^2 [22].

The flexural strength analysis was conducted according to the International Standard Organization (ISO-20795-1) using the ElectroPuls System (E300 Instron, Norwood, MA, USA) operated by the Bluehill software program (Instron Coporation, Norwood, MA). Flexural strength was conducted using the 3 point bending methodology (specimen dimension, length; 65 ± 0.1 mm x width 10 ± 0.1 mm x height: 3 mm ± 0.1 mm) ($n = 5$). Acrylic molds were used covered in commercially available Vaseline to facilitate retrieval. The specimens were compressed in between two glass slides after setting they were retrieved from the mold and polished subsequently (3 μm diamond polishing MetaDi polycrystalline diamond suspension, Buehler). Specimens were stored in distilled water at room temperature (RT). Prior to testing they were taken out and air dried. They were then placed on a support span with a distance of 50 mm and a loading rate of 3 mm / min was applied until fracture using a 1kN load cell. Flexural strength and flexural modulus were calculated using the formula below (2) and (3).

$$Flexural\ load\ MPa = \frac{3PL}{2bd^2} \tag{2}$$

$$Flexural\ modulus\ (MPa) = \frac{PL^3}{4Ybd^3} \tag{3}$$

Whereby P is denoted as the maximum load (N), L is the span (50 mm), b is the width (10 mm) and d is the specimen thickness (3 mm) and Y is the recorded deflection when the load is applied in the middle of the beam.

Specimen dimension for the compressive test were 6 ± 0.1 mm in height and 4 ± 0.1 mm in diameter ($n = 5$). The specimens were prepared using an acrylic mold and glass slides as mentioned previously. Set specimens were stored in distilled water in an incubator at 37 °C. The specimens were placed such that the flat ends were between the plates of the Instron testing machine (ElectroPuls System (E300 Instron, Norwood, MA, USA). The compressive load was applied along the long axis of the specimens with a cross head speed of 3 mm / min using a 1kN load cell. The compressive strength was calculated using the below formula no (4).

$$C = \frac{4p}{\pi\ d^2} \tag{4}$$

Where p is the maximum force applied at the point of fracture and d is the diameter of the specimen [23].

Contact angle

The surface wettability of the prepared specimens ($n = 3$) was evaluated by a polar liquid (distilled water) for contact angle (CA) measurements by adapting a previously reported protocol [24]. A drop of distilled water (3 μL) was added on specimen surfaces at 20 °C. The contact angle was measured by the sessile drop method using a drop shape analyzer (DSA100B; Krüss, Hamburg, Germany). The Krüss drop shape analysis program (ADVANCE 1.7.2.1; Krüss, Hamburg, Germany), determined the contact angle in two steps. In the first step, the drop image was subjected to a gray level analysis. The result was an optically determined contour line around the phase boundary in the drop image. In the second step, this drop contour was calculated mathematically. The contact angle was obtained from the angle between the drop contour function and sample surface. To minimize experimental error, three readings were performed for each specimen and their average value reported. Range of results was from 0 to 180°. To determine the dynamics of CA change with time, the shape of the liquid droplet was recorded by the camera starting from second zero until 5 min with a resolution of 0.01° and accuracy of 0.1° [24].

Degree of conversion

Degree of conversion was conducted according the a previously reported methodology by Khuraif et al. [25]. Absorbance peaks were collected before curing from 10 scans at a resolution of 4 cm^{-1}, over a range of 4,000–300 cm^{-1}, acquired with a Fourier Transform Infrared Spectrophotometer (Bruker Tensor 27, Bruker Optics Ltd, Germany) operating in absorbance mode. The liquid monomer was analyzed using a polyethylene film. Whilst the control and experimental specimens were prepared and placed on the diamond crystal. Small quantity of the specimens were places on the crystal that was enough to cover the space for IR detection. Scans were conducted after every minute till 10 min. The percentage of the unreacted carbon-carbon double bonds (% C = C) was determined from the ratio of absorbance intensities of aliphatic C = C stretching vibrations at 1638 cm^{-1} (Stretching vibration of methacrylate group) and aromatic C = O stretching vibrations at 1720 cm^{-1} to an internal standard before and after curing of the specimen. The degree of conversion was calculated according to the following equation used by Lohbauer et al. [26].

$$Degree\ of\ conversion\ (\%) = \begin{bmatrix} 1 - (A1638/A1720)\ polymerized \\ (A1638/A1720)\ unpolymerized \end{bmatrix} x\ 100$$

Atomic force microscopy (AFM)

Surface topography and roughness of the control and experimental specimens were analysed using an Atomic force microscopy (AFM) ($n = 5$). AFM can provide very high resolution images and 3 dimensional representation of specimens. Polishing of the specimens was done using 3 μm diamond polishing paste (MetaDi polycrystalline diamond suspension, Buehler, IL, USA) Scans of the polished surfaces were performed using AFM (MFP-3D Asylum Oxford Scientific UK) configured as a bimodal nanomechanical force microscope over different areas. The resolution of the AFM was set to capture 256 data points, irrespective of the scan range resulting in 262,144 data points per scanned area. With the 1 × 1 μm scanned image the. The average surface roughness was calculated for all groups and each specimens was scanned at five different regions.

Antimicrobial efficacy test

The experiment was conducted using the *Candida albicans* reference strain (ATCC 90029). The yeast suspension was prepared following the method described by Silva et al., [27]. Briefly, the yeast strain was cultured by inoculating it onto Sabouraud Dextrose Agar (SDA) and incubating at 37 °C for 24 h. A yeast suspension was prepared from the overnight fresh culture by taking a loopful of the growth and inoculating it into yeast nitrogen base (YNB) broth, supplemented with 50 mM glucose. After 18 to 20 h of incubation, the cells were washed twice with PBS and resuspended in YNB. The turbidity of the *C. albicans* standard strain was then adjusted to 10^7 cells/mL using a McFarland densitometer (BioSan, Ratsupites iela 7 k-2, Riga, Latvia).

Biofilms were formed on PMMA surfaces that were placed in presterilized flat-bottomed 24-well microtiter plates (IWAKI, Tokyo, Japan). For the adhesion phase, 2.0 mL aliquots of standard yeast cell suspensions were deposited into each well with a single disc and incubated at 37 °C for 90 min in an orbital shaker at 75 rpm. Following the adhesion phase, the cell solution was carefully removed by aspiration and each specimen was further rinsed twice with PBS. To achieve the biofilm phase, each well was supplied with 2.0 mL of freshly prepared YNB containing 100 mM glucose. The plates were transferred to an incubator at a temperature of 37 °C placed on an orbital shaker at 75 rpm for 24 h. Following the 24-h incubation, the solution was remove and the specimens were rinsed with PBS and MTT assay was conducted using the MTT cell proliferation kit (Roche Diagnostics GmbH, Germany). A known volume of the MTT labelling reagent was added to each well and incubated for 4 h. At the end of the incubation period a known volume of the solubilization solution was added to each well and incubated overnight and colorimetric absorbance was measured at 580 nm (reference wavelength at 650 nm) using a plate reader (CLARIOstar® BMG Labtech, GmbH, Germany).

Scanning Electron microscopy (SEM)

Scanning electron microscopy (SEM) was used to visualize the cells on the specimens. The specimens were fixed with 3% paraformaldehyde in PBS for 2 h, followed by refrigeration overnight. They were then treated with 1% osmium tetraoxide for 2 h and dehydrated by sequential exposure to increasing concentrations of ethanol for 10 min each. Subsequently they were air dried and mounted on aluminum stubs with carbon double adhesive tape and sputter coated under vacuum with gold (JFC-1600, JEOL, Japan). Then the specimens were stored in a desiccator until examination under SEM (JSM- InTouch Scope 200, Jeol, Japan) with an accelerating voltage of 15 kV and a working distance of 10.8 mm at different magnifications.

Statistical analysis

The data is presented as mean ± standard deviation (SD). For the microhardness, flexural strength, flexural modulus, compressive strength, contact angle, and degree of conversion, the data were checked for normality distribution using Shapiro-Wilk test. The statistical significant in between the groups was identified using ANOVA followed by the a Tukey's post hoc test for pair wise comparison at a statistical significance of $p \leq 0.05$. A two-way ANOVA was conducted for the degree of conversion to compare the effect of time intervals and groups. The analysis of the statistical data was done using GraphPad Prism Software (Version 8.0).

Results

The microhardness, flexural strength, flexural modulus and compressive strength of the control and experimental specimens are presented in Fig. 2a to c. Significant difference was observed in the microhardness values in between G1 (15.91 ± 1.57 HV) and G2 (17.67 ± 2.41 HV) ($p > 0.001$). A statistically significant difference was also observed in between G3 (15.59 ± 1.70 HV) and G4 (17.76 ± 2.35) HV) ($p < 0.0001$). No significant differences were noted in between G1 and G3. The obtained results from the flexural strength revealed that all experimental groups had efficiently fulfilled the minimum required strength (ISO 20795-1:2013) of denture base materials ($>$ 60 MPa). The addition of 2.5 wt % nGO revealed the highest flexural strength (70.83 ± 12.51 MPa) but this was not significant compared to other groups. The addition of 1 wt % BN showed less increment in flexural strength which was also not significant compared to other groups. Unlike flexural strength, flexural modulus displayed a different trend with G2 showing the highest modulus (3216.5 ± 902.87 MPa). The highest compressive strength was observed for G4 (58.34 ± 2.53 MPa), followed by G1, G2 and G3 respectively. The lowest was noted for G3 (50.25 ± 3.20 MPa).

Contact angle

Figure 3 shows that the incorporation of 2.5% of nGO (G2) and 1% hBN (G3) into the PMMA increased the contact angle compared to control (G1) with the highest contact angle noted in G2 (84.09° ± 1.49). However, G4 had the lowest contact angle (61.4° ± 2.36). The increase in contact angle in G2 and G3 compared to the unmodified PMMA was statistically significant ($P < 0.05$). This means that the addition of 2.5% nGO and 1% hBN into PMMA significantly increased the wettability of the acrylic. No significant difference in contact angle were noted in between G2 and G3. The synergistic addition of 2.5% nGO and 1% hBN (G4) significantly reduced the contact angle and increased the hydrophilicity of PMMA compared to G1, G2, and G3.

Degree of conversion

Spectroscopic investigation conducted to analyze the chemical spectra after nanoparticle incorporation and degree of conversion results are shown in Fig. 4a to c and peak identifications are shown in Table 1. FTIR analysis

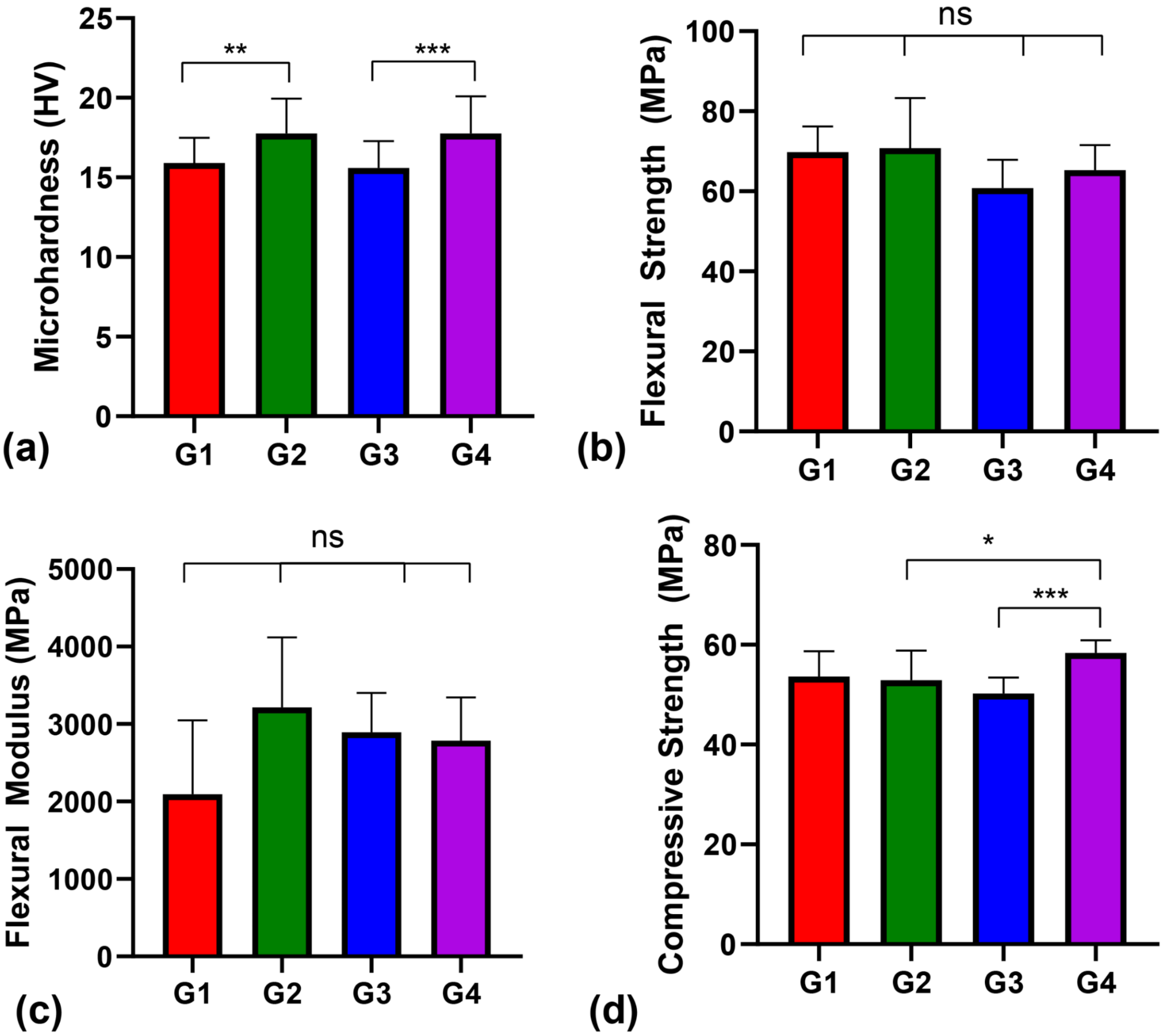

Fig. 2 Bar graphs demonstrating (**a**) Microhardness (**b**) Flexural Strength, (**c**) Flexural Modulus and (**d**) Compressive strength. Values shown are mean ± SD of G1, G2, G3 and G4. (. ** $p > 0.001$, *** $p < 0.0001$)

revealed differences between the unmodified PMMA (G1) and the reinforced PMMA (G2, G3, and G4). The peak heights at 1720 cm^{-1} and 1638 cm^{-1} wavelengths were used for the calculation of the DC. The FTIR spectra of PMMA samples show alpha methyl, ester methyl, methylene C-H stretching (3100–2800 cm^{-1}) and bending mode (1500–1350 cm^{-1}) The carbonyl stretching band can be observed at 1720 cm^{-1}, this shows a sharp peak that indicates the axial deformation of the C = O group of the ester group. Three other bands around 1350 – 1100 region are assigned to ester group stretching vibrations, or to couples C-O and antisymmetric C-C-O stretching at 1241 cm^{-1}. At 1196 and 1157 cm^{-1} skeletal vibrations coupled with C-H deformations can be noticed. Peak at 1638 is attributed to C = C connection vibration, indicating the presence of unreacted C = C double bonds.

The DC values from 0 min to 10 min for each of the four groups (Fig. 4c). At 0 min, the DC of the control group (G1) was 14.19% ± 0.31. With the addition of 1% nGO (G2) and 2.5% hBN (G3), the DC increased to 17.35% ± 0.10 and 20.50% ± 0.23 respectively. On the other hand, when both nanofillers were added together to the PMMA (G4), the DC decreased to 6.23% ± 0.29. The difference in DC that occurred at 0 min was not statistically significant except for G 3 (P-value < 0.05). However, the DC at 2 min in G 4 was statistically significant (P- < 0.05). The DC at 8 min were G1 = 72.94% ± 0.91, G2 = 44.73% ± 0.20, G3 = 45.96% ± 0.17, G4 = 30.25% ± 0.21. At 10 min the percentage of DC were G1 = 84.0% ± 1.0, G2 = 52.88% ±

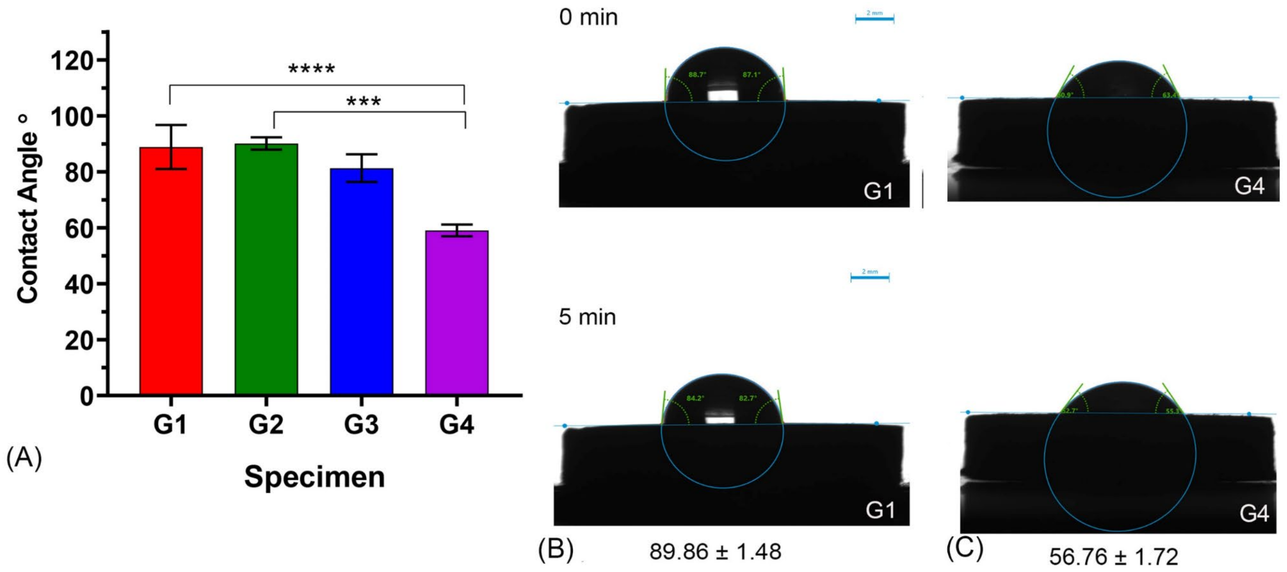

Fig. 3 (**A**) The values of the contact angle of the control and experimental groups (P-value = 0.05). Data shown as mean ± SD; (**B**) Contact angle of group 1 at 0 and 5 min; (**C**) Contact angle of group 4 at 0 and 5 min

0.16, G3 = 52.81% ± 0.15, G4 = 31.73% ± 0.25. When comparing G 3 and 4 to the control group at 8 and 10 min, the decrease in the DC in both groups was statistically significant ($p < 0.05$), but the changes that occurred in G 2 were not statistically significant (P-value > 0.05).

Three dimensional images reconstructed by AFM represent the surface microarchitecture of control and experimental specimens after reinforcing them with nGO and hBN (Fig. 5b, c, d and e). The surface roughness of the specimens is shown in Fig. 5a. A statistically significant difference was observed in between G1 (4.11 ± 1.81 nm) and G3 (13.59 ± 5.99 nm) ($p < 0.0001$). Significant difference was also noted between G2 (6.87 ± 2.24 nm) and G3 (** $p > 0.001$). Addition of hBN significantly increased the roughness whereas the control G1 had the least roughness values. The representative three dimensional images depicted in Fig. 5b to e. A relatively flat and clear surface can be observed with the control unmodified specimen. The addition of nanoparticles resulted in elevated notches on the surface. Which indicated the presence of nanoparticles. Increase in the height can be attributed to agglomeration which can also be noted in G2, G3 and G4 specimens.

Results from the assay antimicrobial efficacy test are shown in Fig. 6a. A significant difference was observed in between G1 and G2 ($p < 0.05$). No significant influence on the *C.albicans* biofilm formation was observed in other groups. Scanning electron microscopy images of the representative groups are also shown in Fig. 6b, c, d and e. *C.albicans* can be observed adhering to the surface of each groups.

Discussion

Contemporary dentistry is facing a significant challenge due to the increment in the number of aging population worldwide. This has led to heightened demands for dental interventions amongst geriatric populations. This is due to their economic and other medical reasons. Researchers are pushing the boundaries of nanotechnology and science to innovate in order to overcome drawbacks of existing biomaterials with respect to denture fractures and microbial adhesion [15]. The emergence of hBN as a novel analogue to graphene has sparked considerable research interests as well [7, 18, 28]. However, there are limited studies in dental applications that dwell into the impact of using nGO and hBN alone or in combination. Previous reports have suggested that a combination of two or more materials with different composition, morphology and characteristics can lead to products with customized physical, chemical and biological properties [15]. In our study, we selected 2.5 wt % nGO and 1 wt% hBN as reinforcing agents based on research and their specific properties. Lee et al. reported a concentration of 2 wt% as an additive in PMMA [3]. Given that nGO has shown to function as a reinforcing agent as lower concentration 2.5 wt% was used as the optimal amount in the current investigation. As for hBN, although studies have explored lower concentrations of 0.8 [29] and 1 wt% [7], we opted for 1 wt% to not only mask the darkness of nGO but also to enhance the physiochemical and mechanical properties. Based on the results of the current study, the null hypothesis had to be rejected, since there were statistically significant difference in surface microhardness, compression strength, contact angle and degree of

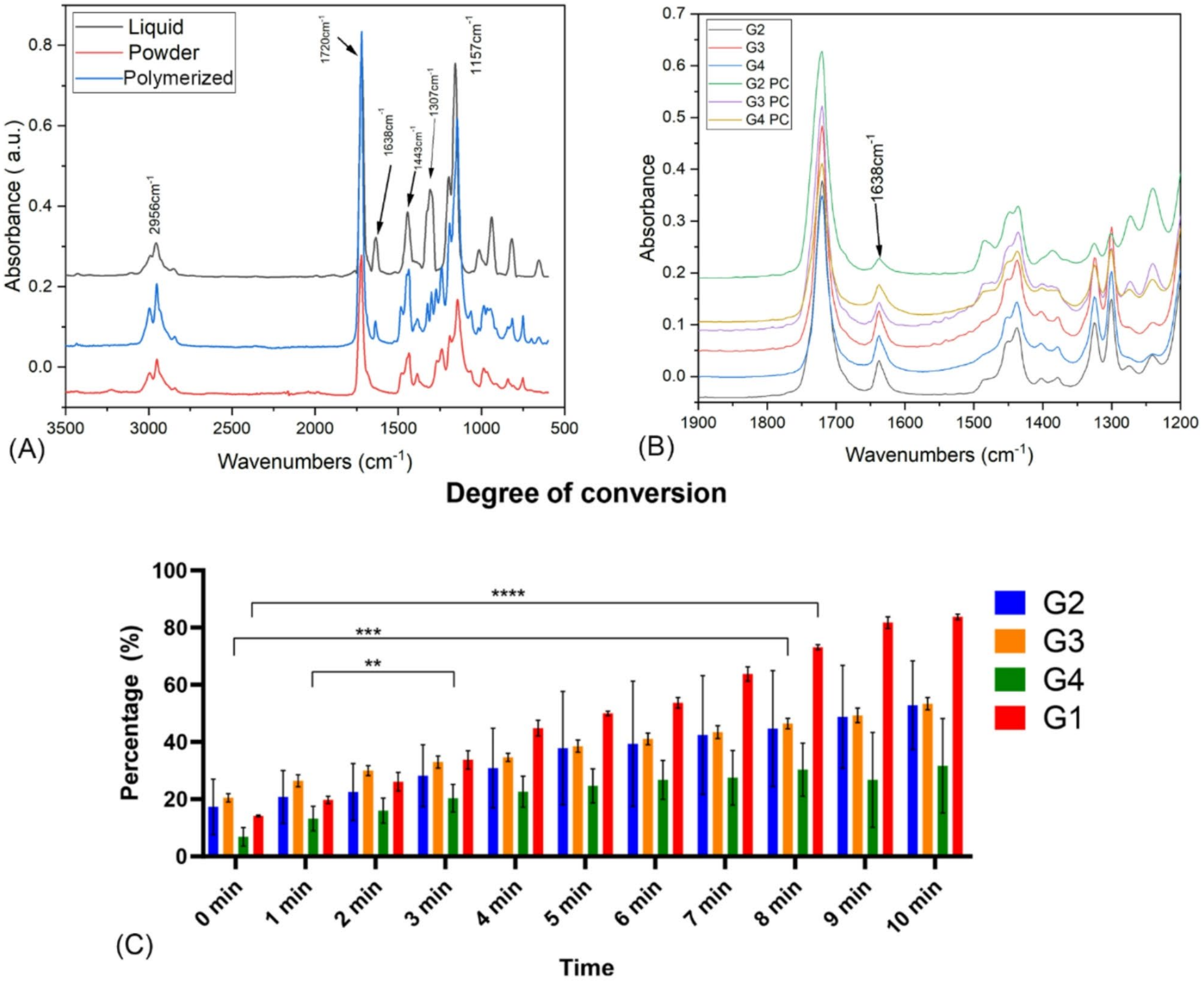

Fig. 4 (**A**) Representative image of FTIR spectra of liquid monomer, powder and polymerized, depicting peaks at 1720 and 1638 for measuring the area in order to calculate the degree of conversion (**B**) representative spectra of groups G2, G3 and G4 at 0 min and after 10 min of mixing; (**C**) Degree of conversion in percentage plotted against time point from all groups with mean and SD. ** $p > 0.001$, **** $p < 0.0001$

conversion of the specimens with nGO, hBN alone and in combination vs. control specimens (G1).

The mechanical properties of the PMMA specimens were systematically tested. Surface microhardness of dental prosthesis are correlated to their wear resistance during the clinical service. Results from the microhardness observed in the current study could be attributed to the presence of nGO, since it is well reported to play a pivotal role in crack deflection and bridging when incorporated into a matrix [3]. Contrary to the current finding doping of PMMA with graphene nanofibers have reported no significant changes with respect to microhardness and surface roughness [16]. Whilst there are mixed reports about the microhardness with graphene reinforcement, a study reported that the addition of 0.15 mg and 0.35 mg of hBN nanosheets along with silver nanoparticles increased microhardness to 194 MPa and 189 MPa respectively [19]. With respect to the results of flexural strength and flexural modulus, no negative impact was observed. According to the international standard for polymer materials and ISO 20795-1:2013 for denture base polymers, the standard states that acrylic resin should achieve no less than 60 MPa. However, G3 (1% hBN) displayed the lowest flexural strength. These findings indicated that there might be lack of chemical crosslinking in between PMMA and hBN matrix [3]. The flexural modulus represents the materials rigidity. Results revealed that all tested specimens met the ISO standards with G2 showing the highest modulus (3.2 GPa). Although hBN is known to effect mechanical integrity since it can trigger a strong interaction with polymers via π- π interaction, polarized nature of hBN bonding or high specific area [18]. The compressive strength analysis revealed a viscoplastic behaviour with

Table 1 Peak identification of monomer and PMMA peaks depicting the peaks shifts

MMA (cm^{-1})	PMMA (cm^{-1})	PEAK IDENTIFICATION
2989	2954	Axial deformation of the C-H bond of the -CH_3 group
2954	2923	Axial deformation of the C-H bond of the -CH_2 group
1719	1720	Axial deformation of the C=O group of the ester group
1635	1637	C=C connection vibration
1438	1402	Symmetrical angular deformation of the group -CH_2
1380	1377	Angular deformation of the -CH_3 group
1301	1280	C-O vibration of the trans-conformation ester group
1191	1196	Vibration of the trans-conformation group -O-CH_3
—	1158	C-C vibration of polymer chain
750	750	Asymmetrical angular deformation of the CH_2 group

a considerable amount of plastic deformation. As the strain rate increased an extended roll-over phenomenon was observed for all specimens [30]. Further studies are needed for optimizing salinization of nGO and hBN for improving mechanical properties.

nGO and hBN have inherently rough surface at the nanoscale [31]. When incorporated into PMMA they can increase the overall roughness of the composite materials. A rougher surface typically enhances the wettability by aiding in more sites for liquid adhesion [32]. Furthermore, nGO and hBN inherently have high surface energies due to their chemical compositions and functional groups [31]. When added to PMMA these materials may increase the overall surface energy of the composite, which can also enhance the wettability. The synergistic effect of nGO and hBN addition can contribute to the results observed in the current study. This can be correlated to the fact that when combined these materials can have a more pronounced effect to enhance the wettability compared to the materials when they are added as a reinforcing agent alone to PMMA.

Spectroscopic investigation were conducted to reveal chemical alterations in the pure and experimental specimens. The spectral data revealed that no significant

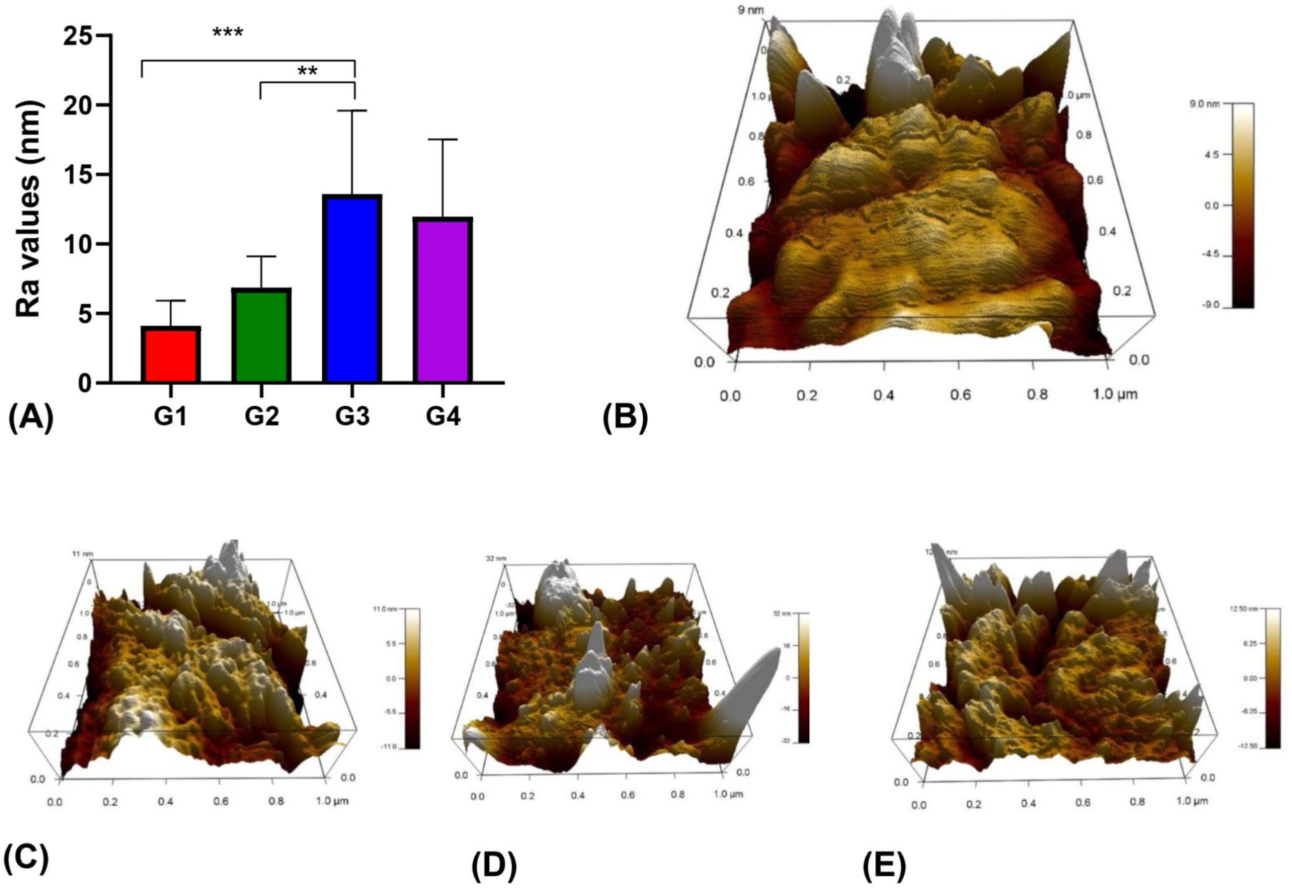

Fig. 5 AFM represents quantitative as well as qualitative data about the effect of reinforcing acrylic resin with different nanoparticles.(**A**) The surface roughness values in nanometers are shown for G1, G2, G3 and G4. Values are shown as mean and SD, statistically significant difference is denoted as, ** $p > 0.001$, **** $p < 0.0001$. Representative images of the morphological surface of the examined groups are also shown.(**B**) G1, (**C**) G2, (**D**) G3, and (**E**) G4

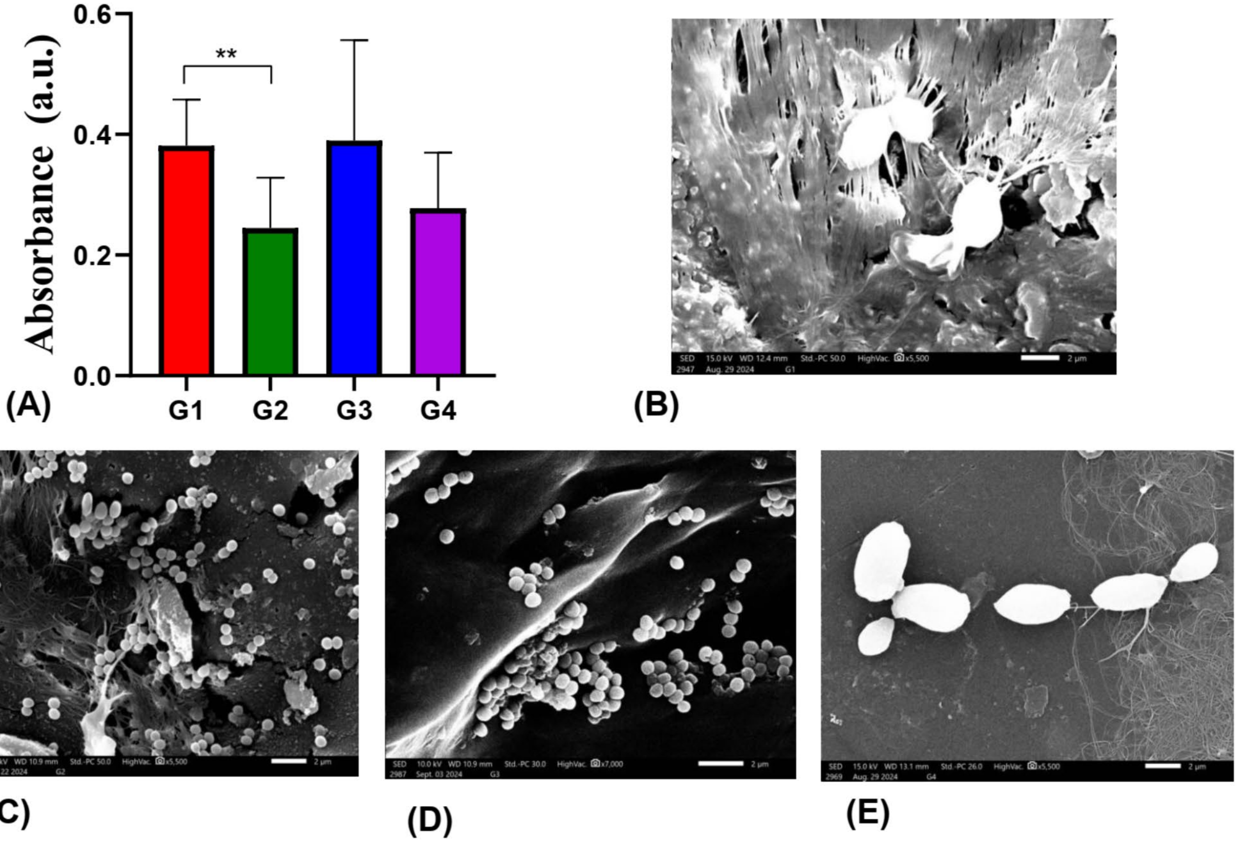

Fig. 6 Antimicrobial efficacy test of nGO and hBN incorporated PMMA against *C.albicans*. After seeding for 24 h the levels of attachment were determined using MTT assays, values presented are mean ± SD, statistically significant difference is denoted as asterisk (**) $p > 0.001$ (**a**). Representative scanning electron microscopy images showing the morphology of *C.albicans* on the specimens (**b, c d** and **e**). All images are scaled at 2 µm

alterations and lack of new peak formations or shifting. The absence of these chemical alterations with respect to graphene have also been reported previously [10, 16]. Indicating that there is possibly physical interactions in between the nanomaterials and PMMA. Alternatively this could be due to homogeneous dispersion of a shallow concentration of nGO and hBN within the PMMA matrix [16]. Besides physical interaction, there is a possibility that nGO and hBN may interact chemically with PMMA by altering its properties. More specifically functional groups on the nano-materials can form bonds or interactions with PMMA molecules. nGO can form hydrogen bonds between PMMA and functional groups in nGO, due to the presence of the carbonyl region which can interact with oxygenated groups on the nGO surface. If higher concentration of nGO is added then the C = O fraction of PMMA is bonded by hydrogen bonding This consequently synergizes to create a toughening mechanism, such as crack deflection [33]. The degree of conversion is direct proportionality with mechanical, thermal and chemical properties. Higher DC polymers generally exhibit greater stiffness and strength [34]. Moreover, they are less likely to undergo deformation, cracking or breakdown. In agreement with the study conducted by Alanasy et al., with the addition of hBN the DC% decreased; however, the concentration used was different (0.3% and 0.5%), and the decrease was not statistically significant [3]. Perhaps a higher concentration of hBN equal to that added for nGO could have a more pronounced effect on the degree of conversion. In order to gain more insights into the polymerization kinetics it would be better to conducted characterization techniques like thermogravimetric analysis, differential scanning calorimetry, dynamic mechanical analysis or gel permeation chromatography. The results of DC are also in agreement to the investigation conducted by Aati et al. [10]. They also observed a reduction in the degree of conversion when 0.05 and more nGO was added (85 – 82%). The higher values could be due to the use do a 3 D printed acrylic resin for their study. Contrary to the results observed in the current study, another investigation showed that nGO addition improved the curing behavior of the epoxy resin by acting as aa catalyst [16].

Surface roughness is a pivotal aspect to be considered when fabricating a dental restoration. Reports suggest that roughness and shape of surfaces affect aesthetics and biomechanical properties of prosthesis. The addition of nGO alone resulted in relative increase in surface roughness due to its higher surface area, inconsistent thickness and shape of the nGO. The increased roughness of G3 could be due to structural mismatch between the nGO and hBN, that could results in a more complex surface structure due to potential agglomeration or may be a mismatch in the bonding. Uneven distribution can also cause microscopic irregularities. An added advantage of this nanoscale roughness of specimens with nGO and hBN could be an enhancement in mechanical interlocking with polymer chains [35]. Nevertheless the surface roughness values stayed below the suggested threshold of dental biomaterials (0.2 µm) that contribute to decreasing the accumulation of debris or biofilm adhesion as well [36]. PMMA surfaces are well reported to be prone to *C.albicans* adhesion and colonization which are correlated with severe local and systemic infections in denture wearing patients [37]. With respect to the results of the microbial susceptibility test a number of studies have shown an antibiofilm effect of nGO [38] and hBN [39]. Ionescu et al. reported that presence of graphene in PMMA reduced biofilm formation. This was also observed in the current investigation, whereby significant differences were noted in between control G1 and G2 group. The process of microbial adhesion is a much more complex phenomenon and it still no fully understood [40]. It encompasses surface characteristics like nano-roughness, topography and surface free energy. The reduction in the biofilm could be related to the physical disruption of the membrane of cell wall and oxidative stress induction, resulting in microbial inhibition [16]. Needless to say, these results require a confirmation from in-vivo clinical studies and must be considered within their limitations.

Although PMMA a relatively affordable biomaterial, graphene oxide and boron nitride are expensive nanomaterials, primarily due to their production. This aspect need to considered when synthesizing novel materials for the wider clinical impact. However these high costs can be offset by the improvements in the materials properties that might offer longer lasting products, which could be cost effect in the long term. When adding fillers to the polymer matrix, it is important to ensure that the fillers are uniformly dispersed throughout the matrix in order to have accurate results when the mechanical and chemical tests are done, especially when using graphene because it tends to agglomerate. This agglomeration is caused by the intrinsic van der Waals forces of the graphene [5]. With ultrasonic mixing, the percent of agglomeration tends to decrease. So, one of the limitations of our study is the use of hand mixing instead of the ultrasonic mixing. Whilst the current investigation provides valuable insights into the effect of novel nanoparticles like nGO and hBN, there are additional avenues for future research that could further enhance our understanding of these biomaterials. Particularly, evaluating viscosity, color stability, thermal properties of modified denture resin, such as glass transition temperature and coefficient of thermal expansion would aid in a more comprehensive understanding of how these nanoparticles influence biomaterials under different temperature conditions. Additionally scanning electron microscopy could also be employed to investigate the ultrastructural morphology and dispersion of nanoparticles within the resin matrix. Another limitation could be curing the resin under ambient room temperature. In future it can be considered to cure the resin under pressure at a slightly elevated temperature for 15 to 15 min this might affect the gas bubble formation within the curing resin. Therefore the use of nanoparticle in the form of nGO and hBN could have a positive impact on the properties, but the risks and benefits should be carefully taken into considerations and safety standards should also be adhered.

Conclusion

The current study is suggestive of the fact that nGO and hBN can be used as either alone of synergistically as reinforcing agents in PMMA denture acrylic resin. The expected increment in the properties could enhance the longevity of denture, ultimately resulting in a better patient satisfaction, reduced maintenance costs and lesser complications associated with the long term use of these materials. Future work could focus on optimizing the composition and processing conditions to maximize mechanical and functional properties while minimizing negative impacts physiochemical performance and microbial adhesion. For clinicians, this delivers an opportunity to give more durable and personalized dentures that can address functional and aesthetic concern. Overall enhancing the quality of care in Prosthodontics.

Acknowledgements

The authors would like to acknowledge Dental Biomaterials research lab, and Grant no. SRUL 01/14, GS 01/05. Research Core Facility (GM 01/15) and Jessy Matthew of the Electron Microscopy Unit (EMU) at the Faculty of Medicine, Kuwait University. The authors would also like to thank Sreeja Saji, Mohammad Arshad, Thulasi, Priya Hasila, Suma and Dr. Nada Mostafa for FTIR analysis.

Author contributions

H.A, R. A and S.S.B.Q led the writing and did most of the experiments. S.S.B.Q and UD critically revised the manuscript and analyzed the experimental data. M.A did experimental work on the microbiological part. S.S.B.Q and u.D reviewed the manuscript and did the experimental part. MA critically reviewed the manuscript. All authors have read and agreed to manuscript submission.

Funding

This research did not receive any specific grant from funding agencies in the public, commercial, or not-for-profit sectors.

Data availability

The data that support the findings of this study are available from the corresponding author upon reasonable request.

Declarations

Ethical approval and consent to participate
All methods were performed in line with the relevant guidelines and regulations. This study is a laboratory based study and does not involve clinical trial. Therefore, no clinician trial number has been assigned.

Consent for publication
Not applicable.

Competing interests
The authors declare no competing interests.

Received: 23 September 2024 / Accepted: 11 April 2025

References

1. An J, Chen C, Xu B. Preparation of arginine-loaded mesoporous silica nanoparticles (Arg@MSNs) to improve the mechanical and antibacterial properties of denture base resin. The Journal of Prosthetic Dentistry 2024, 131(1):165.e161-165.e169.
2. Bangera MK, Kotian R. Effect of titanium dioxide nanoparticle reinforcement on flexural strength of denture base resin: A systematic review and meta-analysis. Japanese Dent Sci Rev. 2020;56(1):68–76.
3. Lee J-H, Jo J-K, Kim D-A, Patel KD, Kim H-W, Lee H-H. Nano-graphene oxide incorporated into PMMA resin to prevent microbial adhesion. Dent Mater. 2018;34(4):e63–72.
4. Nejatian T, Sefat F, Johnson T. Impact of packing and processing technique on mechanical properties of acrylic denture base materials. Materials. 2015;8(5):2093–109.
5. Raszewski Z, Chojnacka K, Mikulewicz M. Preparation and characterization of acrylic resins with bioactive glasses. Sci Rep. 2022;12(1):16624.
6. Vallittu PK. Some aspects of the tensile strength of unidirectional glass fibre–polymethyl methacrylate composite used in dentures. J Rehabil. 1998;25(2):100–5.
7. Li M, Wang S, Li R, Wang Y, Fan X, Gong W, Ma Y. The mechanical and antibacterial properties of Boron nitride/silver nanocomposite enhanced polymethyl methacrylate resin for application in oral denture bases. Biomimetics (Basel, Switzerland) 2022, 7(3).
8. Kaur L, Aras MA, Chitre V, Nagarsekar A, Ferreira AN. Evaluation and comparison of flexural strength, surface roughness and porosity percentage of denture base resins incorporated with thymoquinone and silver nano-antimicrobial agents-an in vitro study. J Oral Biology Craniofac Res. 2022;12(5):716–20.
9. Gad MM, Abualsaud R, Al-Thobity AM, Baba NZ, Al-Harbi FA. Influence of addition of different nanoparticles on the surface properties of Poly(methylmethacrylate) denture base material. J Prosthodont. 2020;29(5):422–8.
10. Aati S, Chauhan A, Shrestha B, Rajan SM, Aati H, Fawzy A. Development of 3D printed dental resin nanocomposite with graphene nanoplatelets enhanced mechanical properties and induced drug-free antimicrobial activity. Dent Mater. 2022;38(12):1921–33.
11. Aldoasri MA, Alsaud KBB, Othman A, Al-Hindawi M, Faisal NH, Ahmed R, Michael FM, Krishnan MR, Alsharaeh E. Microwave irradiation synthesis and characterization of Reduced-(Graphene Oxide-(Polystyrene-Polymethyl Methacrylate))/Silver Nanoparticle Nanocomposites and their Anti-Microbial Activity. Polymers 2020, 12(5).
12. Li M, Wang S, Li R, Wang Y, Fan X, Gong W, Ma Y. The Mechanical and Antibacterial Properties of Boron Nitride/Silver Nanocomposite Enhanced Polymethyl Methacrylate Resin for Application in Oral Denture Bases. Biomimetics 2022, 7(3):138.
13. Yang G, Li L, Lee WB, Ng MC. Structure of graphene and its disorders: a review. Sci Technol Adv Mater. 2018;19(1):613–48.
14. Rosa V, Xie H, Dubey N, Madanagopal TT, Rajan SS, Morin JLP, Islam I, Castro Neto AH. Graphene oxide-based substrate: physical and surface characterization, cytocompatibility and differentiation potential of dental pulp stem cells. Dent Mater. 2016;32(8):1019–25.
15. Bacali C, Baldea I, Moldovan M, Carpa R, Olteanu DE, Filip GA, Nastase V, Lascu L, Badea M, Constantiniuc M, et al. Flexural strength, biocompatibility, and antimicrobial activity of a polymethyl methacrylate denture resin enhanced with graphene and silver nanoparticles. Clin Oral Invest. 2020;24(8):2713–25.
16. Ionescu AC, Brambilla E, Pires PM, López-Castellano A, Alambiaga-Caravaca AM, Lenardi C, Sauro S. Physical-chemical and Microbiological performances of graphene-doped PMMA for CAD/CAM applications before and after accelerated aging protocols. Dent Mater. 2022;38(9):1470–81.
17. Hasan A, Morshed M, Memic A, Hassan S, Webster TJ, Marei HE. Nanoparticles in tissue engineering: applications, challenges and prospects. Int J Nanomed. 2018;13:5637–55.
18. Alansy AS, Saeed TA, Al-Attab R, Guo Y, Yang Y, Liu B, Fan Z. Boron nitride nanosheets modified with zinc oxide nanoparticles as novel fillers of dental resin composite. Dent Mater. 2022;38(10):e266–74.
19. Pullanchiyodan A, Nair S, Surendran K. Silver-Decorated Boron nitride nanosheets as an effective hybrid filler in PMMA for High-Thermal-Conductivity electronic substrates. ACS Omega. 2017;2(12):8825–35.
20. Cheng YK, Campeon BDL, Obata S, Nishina Y. Synergic effect of graphene oxide and Boron nitride on the mechanical properties of polyimide composite films. Nanoscale Adv. 2022;4(10):2339–45.
21. Zhang L, Liu H, Wang Z, Sui W, Gong Y, Cui J, Ao Y, Shang L. Functional Boron nitride/graphene oxide three-dimensional skeleton co-heat transfer epoxy resin composite. J Alloys Compd. 2024;985:173935.
22. AlMatar D, AlSanousi S, Ahmed J, Saad Bin Qasim S. The In-Vitro effect of silver and zinc oxide nanoparticles on fluoride release and microhardness of a Resin-Modified glass ionomer cement. J Inorg Organomet Polym Mater. 2023;33(6):1507–16.
23. Aguirre BC, Chen J-H, Kontogiorgos ED, Murchison DF, Nagy WW. Flexural strength of denture base acrylic resins processed by conventional and CAD-CAM methods. J Prosthet Dent. 2020;123(4):641–6.
24. Qasim SSB, Al-Asfour AA, Abuzayeda M, Mohamed AM, Trajkovski B, Murray CA, Zafiropoulos G-G. Differences in mechanical and physicochemical properties of several PTFE membranes used in guided bone regeneration. Materials. 2023;16(3):904.
25. Kheraif AAAA, Qasim SSB, Ramakrishnaiah R, Rehman, Iu. Effect of different beverages on the color stability and degree of conversion of nano and microhybrid composites. Dent Mater J. 2013;32(2):326–31.
26. Lohbauer U, Rahiotis C, Kramer N, Petschelt A, Eliades G. The effect of different light-curing units on fatigue behavior and degree of conversion of a resin composite. Dent Mater. 2005;21(7):608–15.
27. da Silva WJ, Seneviratne J, Samaranayake LP, Del Bel Cury AA. Bioactivity and architecture of Candida albicans biofilms developed on poly(methyl methacrylate) resin surface. J Biomed Mater Res B Appl Biomater. 2010;94(1):149–56.
28. Alqahtani M. Effect of hexagonal Boron nitride nanopowder reinforcement and mixing methods on physical and mechanical properties of Self-Cured PMMA for dental applications. Materials. 2020;13(10):2323.
29. Wang Y, Xiao S, Lv S, Wang X, Wei R, Ma Y. Mechanical and antimicrobial properties of Boron nitride/methacrylic acid quaternary ammonium composites reinforced dental flowable resins. ACS Biomaterials Sci Eng. 2024;10(3):1796–807.
30. Higgs WA, Lucksanasombool P, Higgs RJ, Swain MV. Comparison of the material properties of PMMA and glass-ionomer based cements for use in orthopaedic surgery. J Mater Sci Mater Med. 2001;12(5):453–60.
31. Sattari Baboukani B, Nalam PC, Komvopoulos K. Nanoscale friction characteristics of layered-structure materials in dry and wet environments. Front Mech Eng 2022, 8.
32. Yang F, McQuain AD, Kumari A, Gundurao D, Liu H, Li L. Understanding the Intrinsic Water Wettability of Hexagonal Boron Nitride. Langmuir 2024, 40(12):6445–6452.
33. Cahyanto A, Martins MVS, Bianchi O, Sudhakaran DP, Sililkas N, Echeverrigaray SG, Rosa V. Graphene oxide increases PMMA's resistance to fatigue and strength degradation. Dent Mater. 2023;39(9):763–9.
34. Aati S, Akram Z, Ngo H, Fawzy AS. Development of 3D printed resin reinforced with modified ZrO2 nanoparticles for long-term provisional dental restorations. Dent Mater. 2021;37(6):e360–74.
35. Degrazia FW, Leitune VCB, Samuel SMW, Collares FM. Boron nitride nanotubes as novel fillers for improving the properties of dental adhesives. J Dent. 2017;62:85–90.
36. Radford DR, Sweet SP, Challacombe SJ, Walter JD. Adherence of Candida albicans to denture-base materials with different surface finishes. J Dent. 1998;26(7):577–83.
37. ten Cate JM, Klis FM, Pereira-Cenci T, Crielaard W, de Groot PW. Molecular and cellular mechanisms that lead to Candida biofilm formation. J Dent Res. 2009;88(2):105–15.

38. Gungordu Er S, Edirisinghe M, Tabish TA. Graphene-Based nanocomposites as antibacterial, antiviral and antifungal agents. Adv Healthc Mater. 2023;12(6):2201523.
39. Kıvanç M, Barutca B, Koparal AT, Göncü Y, Bostancı SH, Ay N. Effects of hexagonal Boron nitride nanoparticles on antimicrobial and antibiofilm activities, cell viability. Mater Sci Engineering: C. 2018;91:115–24.
40. Zhang T, Tremblay P-L. Graphene: an antibacterial agent or a promoter of bacterial proliferation?? iScience 2020, 23(12):101787.

Publisher's note